Helsinki University of Technology, Institute of Mathematics, Research Reports
Teknillisen korkeakoulun matematiikan laitoksen tutkimusraporttisarja
Espoo 2007 A511

A POSTERIORI ESTIMATES FOR THE STOKES EIGENVALUE PROBLEM

Carlo Lovadina Mikko Lyly Rolf Stenberg

TEKNILLINEN KORKEAKOULU
TEKNISKA HÖGSKOLAN
HELSINKI UNIVERSITY OF TECHNOLOGY
TECHNISCHE UNIVERSITÄT HELSINKI
UNIVERSITE DE TECHNOLOGIE D'HELSINKI

Helsinki University of Technology, Institute of Mathematics, Research Reports
Teknillisen korkeakoulun matematiikan laitoksen tutkimusraporttisarja
Espoo 2007 A511

A POSTERIORI ESTIMATES FOR THE STOKES EIGENVALUE PROBLEM

Carlo Lovadina **Mikko Lyly** **Rolf Stenberg**

Helsinki University of Technology
Department of Engineering Physics and Mathematics
Institute of Mathematics

Carlo Lovadina, Mikko Lyly, and Rolf Stenberg: *A posteriori estimates for the Stokes eigenvalue problem*; Helsinki University of Technology, Institute of Mathematics, Research Reports A511 (2007).

Abstract: *We consider the Stokes eigenvalue problem. For the eigenvalues we derive both upper and lower a-posteriori error bounds. The estimates are verified by numerical computations.*

AMS subject classifications: 65N30, 34L15

Keywords: Stokes eigenvalue problem. A-posteriori error estimate. Adaptive computations.

Correspondence

Dipartimento di Matematica, Università di Pavia, and IMATI-CNR
Via Ferrata 1, Pavia I-27100, Italy
`carlo.lovadina@unipv.it`

CSC – Scientific Computing Ltd.
P.O. Box 405, FIN-02101 Espoo, Finland
`mikko.lyly@csc.fi`

Institute of Mathematics, Helsinki University of Technology
P.O.Box 1100, 02015 TKK, Finland
`rolf.stenberg@hut.fi`

ISBN-13 978-951-22-8456-6
ISBN-10 951-22-8456-1

Helsinki University of Technology
Department of Engineering Physics and Mathematics
Institute of Mathematics
P.O. Box 1100, FI-02015 TKK, Finland
email:math@tkk.fi http://math.tkk.fi/

1 Introduction

Regarding a posteriori analysis for finite element methods, most of the results in the literature are addressed to source problems (for example, see [1], [8] and [18], and the references therein). On the contrary, only few results are known about the a posteriori error analysis for eigenvalue problems. We mention here, in a non-exhaustive way, the work [14] for self-adjoint elliptic problems, and the generalisation detailed in [13] to elliptic operators, non necessarily self-adjoint. Moreover, a simple and elegant analysis for the Laplace operator has been performed in [10], while a mixed method has been considered in [9], by exploiting its equivalence with an approximation of non-conforming type (see [2]).

In this paper we present an a posteriori error analysis for the finite element discretization of the Stokes eigenvalue problem, introducing and studying a suitable residual-based error indicator. An outline of the paper is as follows. In Section 2 we briefly recall the eigenvalue problem for the Stokes operator, as well as its finite element discretization. In particular, we focus on stable schemes, which provide reliable approximation for both the source and the eigenvalue problem (see [4]). In Section 3 we introduce the residual-based error indicator. Following the guidelines of [10], we show that the error indicator is equivalent to error, up to higher order terms. Finally, in Section 4 we present some numerical tests for the MINI element, which is a stable element (see [5] and [6], for example), and thus it falls into the category of methods considered. As expected, the numerical experiments confirm our theoretical predictions.

Throughout the paper we will use standard notation for Sobolev norms and seminorms. Moreover, we will denote with C a generic positive constant independent of the mesh parameter h.

2 The Stokes eigenvalue problem and its finite element discretization

Let $\Omega \subset \mathbb{R}^N$ $(N = 2, 3)$ be a Lipschitz domain, with boundary Γ. We are interested in the eigenvalue problem for the Stokes system with homogeneous boundary conditions, i.e.:

$$\begin{cases} \text{Find } (\boldsymbol{u}, p; \lambda), \text{ with } \boldsymbol{u} \neq \boldsymbol{0} \text{ and } \lambda \in \mathbb{R}, \text{ such that} & \\ -\Delta \boldsymbol{u} + \nabla p = \lambda \boldsymbol{u} & \text{in } \Omega, \\ \operatorname{div} \boldsymbol{u} = 0 & \text{in } \Omega, \\ \boldsymbol{u} = \boldsymbol{0} & \text{on } \Gamma. \end{cases} \tag{1}$$

By introducing the bilinear form

$$\mathcal{B}(\boldsymbol{u}, p; \boldsymbol{v}, q) := (\nabla \boldsymbol{u}, \nabla \boldsymbol{v}) - (\operatorname{div} \boldsymbol{v}, p) - (\operatorname{div} \boldsymbol{u}, q), \tag{2}$$

and setting $\boldsymbol{V} = [H^1_0(\Omega)]^N$ and $P = L^2_0(\Omega)$, Problem (1) can be written in a variational form as follows:

$$\begin{cases} \text{Find } (\boldsymbol{u}, p; \lambda) \in (\boldsymbol{V} \times P) \times \mathbb{R}, \text{ with } \boldsymbol{u} \neq \boldsymbol{0}, \text{ such that} \\ \mathcal{B}(\boldsymbol{u}, p; \boldsymbol{v}, q) = \lambda(\boldsymbol{u}, \boldsymbol{v}) \qquad \forall (\boldsymbol{v}, q) \in \boldsymbol{V} \times P. \end{cases} \tag{3}$$

We recall (see, e.g. [5]) that the bilinear form $\mathcal{B}$ is stable, i.e.:

- Given $(\boldsymbol{v}, q) \in \boldsymbol{V} \times P$, there exists $(\boldsymbol{w}, s) \in \boldsymbol{V} \times P$ such that

$$\begin{cases} \|\boldsymbol{w}\|_1 + \|s\|_0 \leq C \\ \|\boldsymbol{v}\|_1 + \|q\|_0 \leq \mathcal{B}(\boldsymbol{v}, q; \boldsymbol{w}, s), \end{cases} \tag{4}$$

and it is continuous, i.e.:

- For every $(\boldsymbol{v}, q), (\boldsymbol{w}, s) \in \boldsymbol{V} \times P$, it holds

$$\mathcal{B}(\boldsymbol{v}, q; \boldsymbol{w}, s) \leq C\left(\|\boldsymbol{v}\|_1 + \|q\|_0\right)\left(\|\boldsymbol{w}\|_1 + \|s\|_0\right). \tag{5}$$

We now turn to the discretization of Problem (3) by finite elements. Let $\{\mathcal{C}_h\}_{h>0}$ be a sequence of decompositions of Ω into elements K, satisfying the usual compatibility conditions (see [7]). We also assume that the family $\{\mathcal{C}_h\}_{h>0}$ is regular, i.e. there exists a constant $\sigma > 0$ such that

$$h_K \leq \sigma \rho_K \qquad \forall\, K \in \mathcal{C}_h, \tag{6}$$

where h_K is the diameter of the element K and ρ_K is the maximum diameter of the circles contained in K. Associated with the mesh $\mathcal{C}_h$, we select finite elements spaces $\boldsymbol{V}_h \subset \boldsymbol{V}$ and $P_h \subset P$, and we consider the discrete Stokes eigenvalue problem:

$$\begin{cases} \text{Find } (\boldsymbol{u}_h, p_h; \lambda_h) \in (\boldsymbol{V}_h \times P_h) \times \mathbb{R}, \text{ with } \boldsymbol{u}_h \neq \boldsymbol{0}, \text{ such that} \\ \mathcal{B}(\boldsymbol{u}_h, p_h; \boldsymbol{v}, q) = \lambda_h(\boldsymbol{u}_h, \boldsymbol{v}) \qquad \forall (\boldsymbol{v}, q) \in \boldsymbol{V}_h \times P_h. \end{cases} \tag{7}$$

We assume that the pair $(\boldsymbol{V}_h, P_h)$ satisfies the following properties:

- (*Inf-sup* condition) There exists $\beta > 0$ independent of h, such that

$$\sup_{\boldsymbol{v}_h \in \boldsymbol{V}_h} \frac{(\operatorname{div} \boldsymbol{v}_h, q_h)}{\|\boldsymbol{v}_h\|_1} \geq \beta \|q_h\|_0 \qquad \forall q_h \in P_h. \tag{8}$$

- Assuming that $\boldsymbol{u} \in [H^{1+r}(\Omega)]^N$ and $p \in H^r(\Omega)$, for some $r \in (0, 1]$, it holds

$$\inf_{\boldsymbol{v}_h \in \boldsymbol{V}_h} \|\boldsymbol{u} - \boldsymbol{v}_h\|_1 \leq Ch^r |\boldsymbol{u}|_{r+1} \tag{9}$$

  and

$$\inf_{q_h \in P_h} \|p - q_h\|_0 \leq Ch^s |p|_r. \tag{10}$$

It is well-known (see [6], for instance) that (8)–(10) imply convergence and stability of the given finite element scheme for the Stokes source problem. It has been proved in [4] that (8)–(10) are sufficient conditions for the convergence of the Stokes eigenvalue problem (7) as well. Indeed, by using the regularity results detailed in, e.g., [12] and [16], and well-established techniques for eigenvalue approximation (see [3], [15] and [4], for example), one has the following result.

Theorem 2.1. *Given an eigenpair $(\boldsymbol{u}, p; \lambda) \in (\boldsymbol{V} \times P) \times \mathbb{R}$, solution of (3), there exists $r \in (0, 1]$ such that $\boldsymbol{u} \in [H^{1+r}(\Omega)]^N$, $p \in H^r(\Omega)$. Furthermore, for every positive $h \leq h_0(\lambda)$, there exists a* discrete *eigenpair $(\boldsymbol{u}_h, p_h; \lambda_h) \in (\boldsymbol{V}_h \times P_h) \times \mathbb{R}$, solution of (7), such that*

$$|\lambda - \lambda_h| \leq C \left(\|\boldsymbol{u} - \boldsymbol{u}_h\|_1 + \|p - p_h\|_0\right)^2 , \tag{11}$$

$$\|\boldsymbol{u} - \boldsymbol{u}_h\|_1 + \|p - p_h\|_0 \leq C h^r \big(\|\boldsymbol{u}\|_{1+r} + \|p\|_r\big), \tag{12}$$

$$\|\boldsymbol{u} - \boldsymbol{u}_h\|_0 \leq C h^{2r} \big(\|\boldsymbol{u}\|_{1+r} + \|p\|_r\big). \tag{13}$$

□

Throughout the rest of the paper, we will denote with

$$e(\boldsymbol{u}) = \boldsymbol{u} - \boldsymbol{u}_h, \qquad e(p) = p - p_h \tag{14}$$

the eigenfunction errors, where $\boldsymbol{u}$, $\boldsymbol{u}_h$, p and p_h are as in Theorem 2.1.

3 A posteriori error analysis

The aim of this section is to introduce a suitable residual-based error estimator for the Stokes eigenvalue problems. To begin, for each element $K \in \mathcal{C}_h$ we introduce the residuals (cf. (1))

$$R_{K,1}(\boldsymbol{u}_h, p_h) = \Delta \boldsymbol{u}_h - \nabla p_h + \lambda_h \boldsymbol{u}_h, \tag{1}$$

$$R_{K,2}(\boldsymbol{u}_h) = \operatorname{div} \boldsymbol{u}_h, \tag{2}$$

$$R_{\partial K}(\boldsymbol{u}_h, p_h) = [\![(\nabla \boldsymbol{u}_h - p_h \boldsymbol{I}) \cdot \boldsymbol{n}_K]\!]_{|\partial K} \ . \tag{3}$$

Accordingly, we define the local error estimator as

$$\eta_K^2 = h_K^2 \|R_{K,1}(\boldsymbol{u}_h, p_h)\|_{0,K}^2 + \|R_{K,2}(\boldsymbol{u}_h)\|_{0,K}^2 + \frac{h_K}{2} \|R_{\partial K}(\boldsymbol{u}_h, p_h)\|_{0,\partial K}^2. \tag{4}$$

Finally, the global error estimator is given by

$$\eta^2 = \sum_{K \in \mathcal{C}_h} \eta_K^2. \tag{5}$$

3.1 Upper bounds

We now provide an upper bound for our error estimator.

Theorem 3.1. *Let* $(\boldsymbol{u}, p; \lambda) \in (\boldsymbol{V} \times P) \times \mathbb{R}$ *be a solution of* (3), *and let* $(\boldsymbol{u}_h, p_h; \lambda_h) \in (\boldsymbol{V}_h \times P_h) \times \mathbb{R}$ *be a solution of* (7), *as in Theorem 2.1. For every positive* $h \le h_0(\lambda)$, *it holds*

$$\|e(\boldsymbol{u})\|_1 + \|e(p)\|_0 \le C\big(\eta + |\lambda - \lambda_h| + \lambda\|\boldsymbol{u} - \boldsymbol{u}_h\|_0\big). \tag{6}$$

Proof. Choose a generic pair $(\boldsymbol{v}, q) \in \boldsymbol{V}_h \times P_h$ as a test function for (3). By subtracting (7) from (3), we get the following error equation

$$\mathcal{B}(e(\boldsymbol{u}), e(p); \boldsymbol{v}, q) = (\lambda \boldsymbol{u} - \lambda_h \boldsymbol{u}_h, \boldsymbol{v}) \qquad \forall (\boldsymbol{v}, q) \in \boldsymbol{V}_h \times P_h \ , \tag{7}$$

where $e(\boldsymbol{u})$ and $e(p)$ are defined as in (14). By the stability of the continuous Stokes problem (cf. (4)), there exists $(\boldsymbol{w}, s) \in \boldsymbol{V} \times P$, with

$$\|\boldsymbol{w}\|_1 + \|s\|_0 \le C \ , \tag{8}$$

such that

$$\|e(\boldsymbol{u})\|_1 + \|e(p)\|_0 \le \mathcal{B}(e(\boldsymbol{u}), e(p); \boldsymbol{w}, s) \ . \tag{9}$$

Let $\boldsymbol{w}^I \in \boldsymbol{V}_h$ be the Clément interpolant of $\boldsymbol{w}$ (cf. e.g. [5, 17]), and let $s^I \in P_h$ be the L^2-projection of s. By using the error equation (7), estimate (9) gives

$$\begin{aligned}\|e(\boldsymbol{u})\|_1 + \|e(p)\|_0 &\le \mathcal{B}(e(\boldsymbol{u}), e(p); \boldsymbol{w} - \boldsymbol{w}^I, s - s^I) + (\lambda \boldsymbol{u} - \lambda_h \boldsymbol{u}_h, \boldsymbol{w}^I) \\ &= \mathcal{B}(e(\boldsymbol{u}), e(p); \boldsymbol{w} - \boldsymbol{w}^I, s - s^I) - (\lambda \boldsymbol{u} - \lambda_h \boldsymbol{u}_h, \boldsymbol{w} - \boldsymbol{w}^I) \\ &\quad + (\lambda \boldsymbol{u} - \lambda_h \boldsymbol{u}_h, \boldsymbol{w}) \ .\end{aligned} \tag{10}$$

Integrating by parts, using the continuous Stokes equations (1), and recalling (1)–(3) we obtain

$$\begin{aligned}&\mathcal{B}(e(\boldsymbol{u}), e(p); \boldsymbol{w} - \boldsymbol{w}^I, s - s^I) - (\lambda \boldsymbol{u} - \lambda_h \boldsymbol{u}_h, \boldsymbol{w} - \boldsymbol{w}^I) \\ &= \sum_{K \in \mathcal{C}_h} \Big\{ (R_{K,1}(\boldsymbol{u}_h, p_h), \boldsymbol{w} - \boldsymbol{w}^I)_K + (R_{K,2}(\boldsymbol{u}_h), s - s^I)_K \\ &\qquad + \frac{1}{2} \langle R_{\partial K}(\boldsymbol{u}_h, p_h), \boldsymbol{w} - \boldsymbol{w}^I \rangle_{\partial K} \Big\} \ ,\end{aligned} \tag{11}$$

where the brackets $\langle \cdot, \cdot \rangle_{\partial K}$ denote the L^2 inner product on the boundary ∂K. Applying the Cauchy-Schwarz inequality to Eq. (11), we obtain

$$\begin{aligned}&\mathcal{B}(e(\boldsymbol{u}), e(p); \boldsymbol{w} - \boldsymbol{w}^I, s - s^I) - (\lambda \boldsymbol{u} - \lambda_h \boldsymbol{u}_h) \\ &\le C \Big\{ \sum_{K \in \mathcal{C}_h} \Big(h_K^{-2} \|\boldsymbol{w} - \boldsymbol{w}^I\|_{0,K}^2 + h_K^{-1} \|\boldsymbol{w} - \boldsymbol{w}^I\|_{0,\partial K}^2 + \|s - s^I\|_{0,K} \Big) \Big\}^{1/2} \times \\ &\Big\{ \sum_{K \in \mathcal{C}_h} \Big(h_K^2 \|R_{K,1}(\boldsymbol{u}_h, p_h)\|_{0,K}^2 + \|R_{K,2}(\boldsymbol{u}_h)\|_{0,\partial K}^2 + \frac{h_K}{2} \|R_{\partial K}(\boldsymbol{u}_h, p_h)\|_{0,\partial K}^2 \Big) \Big\}^{1/2}\end{aligned} \tag{12}$$

Since for the Clément interpolation it holds

$$\Big\{ \sum_{K\in\mathcal{C}_h} \Big(h_K^{-2}\|\boldsymbol{w}-\boldsymbol{w}^I\|_{0,K}^2 + h_K^{-1}\|\boldsymbol{w}-\boldsymbol{w}^I\|_{0,\partial K}^2 \Big) \Big\}^{1/2} \le C\|\boldsymbol{w}\|_1 \ , \tag{13}$$

and for the L^2 projection we have

$$\|s^I\|_0 \le \|s\|_0 \ , \tag{14}$$

the estimates (12), (8) and (5) give

$$\mathcal{B}(e(\boldsymbol{u}), e(p); \boldsymbol{w}-\boldsymbol{w}^I, s-s^I) - (\lambda\boldsymbol{u}-\lambda_h\boldsymbol{u}_h, \boldsymbol{w}-\boldsymbol{w}^I) \le C\eta \ . \tag{15}$$

It remains to estimate the term $(\lambda\boldsymbol{u}-\lambda_h\boldsymbol{u}_h, \boldsymbol{w})$, see (10). We may write

$$\begin{aligned}(\lambda\boldsymbol{u}-\lambda_h\boldsymbol{u}_h, \boldsymbol{w}) &= ((\lambda-\lambda_h)\boldsymbol{u}_h, \boldsymbol{w}) + \lambda((\boldsymbol{u}-\boldsymbol{u}_h), \boldsymbol{w}) \\ &\le |\lambda-\lambda_h|\|\boldsymbol{u}_h\|_0\|\boldsymbol{w}\|_0 + \lambda\|\boldsymbol{u}-\boldsymbol{u}_h\|_0\|\boldsymbol{w}\|_0 \\ &\le C\big(|\lambda-\lambda_h| + \lambda\|\boldsymbol{u}-\boldsymbol{u}_h\|_0\big) \ ,\end{aligned} \tag{16}$$

where we have used (8). Collecting (15) and (16), from (10) we get

$$\|e(\boldsymbol{u})\|_1 + \|e(p)\|_0 \le C\big(\eta + |\lambda-\lambda_h| + \lambda\|\boldsymbol{u}-\boldsymbol{u}_h\|_0\big) \ , \tag{17}$$

i.e. estimate (6). ☐

Corollary 3.1. *For the eigenvalue approximation, it holds*

$$|\lambda-\lambda_h| \le C\big(\eta^2 + |\lambda-\lambda_h|^2 + \lambda^2\|\boldsymbol{u}-\boldsymbol{u}_h\|_0^2\big). \tag{18}$$

Proof. The assertion immediately follows by squaring estimate (6), and using the a priori bound (11) of Theorem 2.1. ☐

Remark 3.1. *In view of Theorem 2.1 the quantities $|\lambda-\lambda_h| + \lambda\|\boldsymbol{u}-\boldsymbol{u}_h\|_0$ in (6) and $|\lambda-\lambda_h|^2 + \lambda^2\|\boldsymbol{u}-\boldsymbol{u}_h\|_0^2$ in (18) are both higher-order terms.*

3.2 Lower bounds

Next, we show a local lower bound on the estimator. We denote with $\omega(K)$ the union of all elements having at least one edge (for $N = 2$) – or one face (for $N = 3$) – in common with K. Similarly, for a given edge (for $N = 2$) E – or face (for $N = 3$) – the set $\omega(E)$ is the union of the elements which contain E.

Theorem 3.2. *Let $(\boldsymbol{u}, p; \lambda) \in (\boldsymbol{V} \times P) \times \mathbb{R}$ be a solution of (3), and let $(\boldsymbol{u}_h, p_h; \lambda_h) \in (\boldsymbol{V}_h \times P_h) \times \mathbb{R}$ be a solution of (7), as in Theorem 2.1. For every positive $h \le h_0(\lambda)$, it holds*

$$\begin{aligned}\eta_K \le C\Big(&\|\nabla e(\boldsymbol{u})\|_{0,\omega(K)} + \|e(p)\|_{0,\omega(K)} \\ &+ \sum_{K'\subset\omega(K)} h_{K'}^{1/2}\big(|\lambda-\lambda_h| + \lambda\|\boldsymbol{u}-\boldsymbol{u}_h\|_{0,K'}\big)\Big).\end{aligned} \tag{19}$$

Proof. We set

$$\boldsymbol{v}_K := h_K^2 b_K R_{K,1}(\boldsymbol{u}_h, p_h) \ , \tag{20}$$

where b_K denotes the standard bubble function of the element K. By recalling (1) and by usual scaling arguments, we get

$$\begin{aligned} Ch_K^2 \|R_{K,1}(\boldsymbol{u}_h, p_h)\|_{0,K}^2 &\le (\Delta \boldsymbol{u}_h - \nabla p_h + \lambda_h \boldsymbol{u}_h, \boldsymbol{v}_K)_K \\ &= \big(\Delta(\boldsymbol{u}_h - \boldsymbol{u}) - \nabla(p_h - p) + \lambda_h \boldsymbol{u}_h - \lambda \boldsymbol{u}, \boldsymbol{v}_K\big)_K \\ &= -\big(\Delta e(\boldsymbol{u}) - \nabla e(p) + \lambda_h \boldsymbol{u}_h - \lambda \boldsymbol{u}, \boldsymbol{v}_K\big)_K, \end{aligned} \tag{21}$$

where we have used $-\Delta \boldsymbol{u} + \nabla p - \lambda \boldsymbol{u} = \boldsymbol{0}$. We have

$$\begin{aligned} -\big(\Delta e(\boldsymbol{u}) - \nabla e(p), \boldsymbol{v}_K\big)_K &= \big(\nabla e(\boldsymbol{u}), \nabla \boldsymbol{v}_K\big)_K - \big(e(p), \operatorname{div} \boldsymbol{v}_K\big)_K \\ &\le C\left(\|\nabla e(\boldsymbol{u})\|_{0,K} + \|e(p)\|_{0,K}\right) \|\nabla \boldsymbol{v}_K\|_{0,K}, \\ &\le C\left(\|\nabla e(\boldsymbol{u})\|_{0,K} + \|e(p)\|_{0,K}\right) h_K \|R_{K,1}(\boldsymbol{u}_h, p_h)\|_{0,K}. \end{aligned} \tag{22}$$

Furthermore, it holds

$$\begin{aligned} (\lambda_h \boldsymbol{u}_h - \lambda \boldsymbol{u}, \boldsymbol{v}_K)_K &= ((\lambda_h - \lambda)\boldsymbol{u}_h, \boldsymbol{v}_K) + \lambda((\boldsymbol{u}_h - \boldsymbol{u}), \boldsymbol{v}_K) \\ &\le \big(|\lambda - \lambda_h| \|\boldsymbol{u}_h\|_{0,K} + \lambda \|\boldsymbol{u} - \boldsymbol{u}_h\|_{0,K}\big) \|\boldsymbol{v}_K\|_{0,K} \\ &\le C\big(|\lambda - \lambda_h| + \lambda \|\boldsymbol{u} - \boldsymbol{u}_h\|_{0,K}\big) \|\boldsymbol{v}_K\|_{0,K} \\ &\le C\big(|\lambda - \lambda_h| + \lambda \|\boldsymbol{u} - \boldsymbol{u}_h\|_{0,K}\big) h_K^2 \|R_{K,1}(\boldsymbol{u}_h, p_h)\|_{0,K}. \end{aligned} \tag{23}$$

From (21)–(23) we get

$$\begin{aligned} h_K \|R_{K,1}(\boldsymbol{u}_h, p_h)\|_{0,K} \le C\big(&\|\nabla e(\boldsymbol{u})\|_{0,K} + \|e(p)\|_{0,K} \\ &+ h_K |\lambda - \lambda_h| + h_K \lambda \|\boldsymbol{u} - \boldsymbol{u}_h\|_{0,K}\big). \end{aligned} \tag{24}$$

To continue, we trivially have

$$\|R_{K,2}(\boldsymbol{u}_h)\|_{0,K} = \|\operatorname{div} \boldsymbol{u}_h\|_{0,K} = \|\operatorname{div} e(\boldsymbol{u})\|_{0,K} \le \sqrt{N} \|\nabla e(\boldsymbol{u})\|_{0,K}. \tag{25}$$

Fix now an edge (for $N = 2$) or a face (for $N = 3$) $E \subset \partial K$. Consider

$$\boldsymbol{\varphi}_E := h_E b_E R_E(\boldsymbol{u}_h, p_h), \tag{26}$$

where h_E is the diameter of E, the function $b_E \in H_0^1(\omega(E))$ is the usual bubble function for E (see [18], for example), and the residual $R_E(\boldsymbol{u}_h, p_h)$ is defined by (cf. also (3))

$$R_E(\boldsymbol{u}_h, p_h) = [\![(\nabla \boldsymbol{u}_h - p_h \boldsymbol{I}) \cdot \boldsymbol{n}_E]\!]_{|E} \, . \tag{27}$$

By standard scaling arguments, using $[\![(\nabla \boldsymbol{u} - p\boldsymbol{I}) \cdot \boldsymbol{n}_E]\!]_{|E} = \boldsymbol{0}$, and integrating by parts, we get

$$\begin{aligned} Ch_E \|R_E(\boldsymbol{u}_h, p_h)\|_{0,E}^2 &\le \langle [\![(\nabla \boldsymbol{u}_h - p_h \boldsymbol{I}) \cdot \boldsymbol{n}_E]\!] \, , \boldsymbol{\varphi}_E \rangle_E \\ &= -\langle [\![(\nabla e(\boldsymbol{u}) - e(p)\boldsymbol{I}) \cdot \boldsymbol{n}_E]\!] \, , \boldsymbol{\varphi}_E \rangle_E \\ &= -\big(\nabla e(\boldsymbol{u}), \nabla \boldsymbol{\varphi}_E\big)_{\omega(E)} + \big(e(p), \operatorname{div} \boldsymbol{\varphi}_E\big)_{\omega(E)} \\ &\quad - \sum_{K \subset \omega(E)} \big(\Delta e(\boldsymbol{u}) - \nabla e(p), \boldsymbol{\varphi}_E\big)_K. \end{aligned} \tag{28}$$

We also have, using again scaling arguments and (26):

$$
\begin{aligned}
-\big(\nabla e(\boldsymbol{u}), \nabla\, \boldsymbol{\varphi}_E\big)_{\omega(E)} &+ \big(e(p), \operatorname{div} \boldsymbol{\varphi}_E\big)_{\omega(E)} \\
&\le C\big(\|\nabla e(\boldsymbol{u})\|_{0,\omega(E)} + \|e(p)\|_{0,\omega(E)}\big)\|\nabla \boldsymbol{\varphi}_E\|_{0,\omega(E)} \\
&\le C\big(\|\nabla e(\boldsymbol{u})\|_{0,\omega(E)} + \|e(p)\|_{0,\omega(E)}\big) h_E^{1/2}\|R_E(\boldsymbol{u}_h, p_h)\|_{0,E}.
\end{aligned}
\tag{29}
$$

Furthermore, it holds

$$
\begin{aligned}
-\sum_{K\subset\omega(E)} &\big(\Delta e(\boldsymbol{u}) - \nabla e(p), \boldsymbol{\varphi}_E\big)_K \\
&= \sum_{K\subset\omega(E)} \left\{\big(R_{K,1}(\boldsymbol{u}_h, p_h), \boldsymbol{\varphi}_E\big)_K + \big(\lambda\boldsymbol{u} - \lambda_h\boldsymbol{u}_h, \boldsymbol{\varphi}_E\big)_K\right\}.
\end{aligned}
\tag{30}
$$

On the one hand we get

$$
\begin{aligned}
\sum_{K\subset\omega(E)} &\big(R_{K,1}(\boldsymbol{u}_h, p_h), \boldsymbol{\varphi}_E\big)_K \\
&\le C\Big(\sum_{K\subset\omega(E)} h_K\|R_{K,1}(\boldsymbol{u}_h, p_h)\|_{0,K}\Big) h_E^{1/2}\|R_E(\boldsymbol{u}_h, p_h)\|_{0,E}.
\end{aligned}
\tag{31}
$$

Similar computations as in (23) show that

$$
\sum_{K\subset\omega(E)} \big(\lambda\boldsymbol{u} - \lambda_h\boldsymbol{u}_h, \boldsymbol{\varphi}_E\big) \le C\big(|\lambda-\lambda_h| + \lambda\|\boldsymbol{u}-\boldsymbol{u}_h\|_{0,\omega(E)}\big) h_E^{3/2}\|R_E(\boldsymbol{u}_h, p_h)\|_{0,E}.
\tag{32}
$$

Therefore, from (30), (31) and (32), we obtain

$$
\begin{aligned}
&-\sum_{K\subset\omega(E)} \big(\Delta e(\boldsymbol{u}) - \nabla e(p), \boldsymbol{\varphi}_E\big)_K \\
&\le C\Big(\sum_{K\subset\omega(E)} h_K\|R_{K,1}(\boldsymbol{u}_h, p_h)\|_{0,K} + h_E^{1/2}\big(|\lambda-\lambda_h| + \lambda\|\boldsymbol{u}-\boldsymbol{u}_h\|_{0,\omega(E)}\big)\Big)\times \\
&\qquad h_E^{1/2}\|R_E(\boldsymbol{u}_h, p_h)\|_{0,E}.
\end{aligned}
\tag{33}
$$

Taking into account estimates (29) and (33), from (28) we infer

$$
\begin{aligned}
&h_E^{1/2}\|R_E(\boldsymbol{u}_h, p_h)\|_{0,E} \\
&\le C\Big(\sum_{K\subset\omega(E)} h_K\|R_{K,1}(\boldsymbol{u}_h, p_h)\|_{0,K} + h_E^{1/2}\big(|\lambda-\lambda_h| + \lambda\|\boldsymbol{u}-\boldsymbol{u}_h\|_{0,\omega(E)}\big)\Big).
\end{aligned}
\tag{34}
$$

Summing over the element edges (for $N = 2$), or faces (for $N = 3$), (34) and the regularity of the mesh $\mathcal{C}_h$ give

$$
\begin{aligned}
&\frac{h_K^{1/2}}{\sqrt{2}}\|R_{\partial K}(\boldsymbol{u}_h, p_h)\|_{0,\partial K} \\
&\le C\sum_{K'\subset\omega(K)} \Big(h_{K'}\|R_{K',1}(\boldsymbol{u}_h, p_h)\|_{0,K'} + h_{K'}^{1/2}\big(|\lambda-\lambda_h| + \lambda\|\boldsymbol{u}-\boldsymbol{u}_h\|_{0,K'}\big)\Big).
\end{aligned}
\tag{35}
$$

By recalling (4), from (24), (25) and (35), we get

$$\eta_K \le C\Big(\|\nabla e(\boldsymbol{u})\|_{0,\omega(K)} + \|e(p)\|_{0,\omega(K)} \\ + \sum_{K'\subset\omega(K)} h_{K'}^{1/2}\big(|\lambda-\lambda_h| + \lambda\|\boldsymbol{u}-\boldsymbol{u}_h\|_{0,K'}\big)\Big), \tag{36}$$

which completes the proof. □

4 Numerical results

Our numerical examples will be given for the two-dimensional problem with the linear triangular MINI-element (see [6], for instance) for which the velocity and pressure spaces are defined as

$$\boldsymbol{V}_h = \{\boldsymbol{v}\in\boldsymbol{V} \mid \boldsymbol{v}_{|K} \in [P_1(K)]^2 \oplus [P_3(K)\cap H_0^1(K)]^2 \ \forall K\in\mathcal{C}_h\} \tag{1}$$

and

$$P_h = \{q \in P\cap H^1(\Omega) \mid q_{|K}\in P_1(K) \ \forall\ K\in\mathcal{C}_h\} \tag{2}$$

where $P_k(K)$ is the space of polynomials of degree k defined on $K\in\mathcal{C}_h$. All the computations have been performed with the open-source finite element software Elmer [11].

4.1 Square domain

In our first example we will consider the square $\Omega = (-1,1)\times(-1,1)$ with homogenous Dirichlet boundary conditions imposed on the velocity. The finite element mesh is obtained by dividing the domain into $2N\times N$ triangles as shown in Figure 1.

In Table 1 we have tabulated the 10 smallest eigenvalues of the Stokes operator as a function of $N\in\{4,8,\dots,128\}$. Our reference solution is given in the last column of the table. The reference has been extrapolated from the numerical results by assuming that the error $|\lambda-\lambda_h|$ behaves as Ch^r for some constants C and r independent of $h=\sqrt{2/N}$.

The relative error $|\lambda-\lambda_h|/\lambda$ with respect to the reference solution is shown in Table 2. In Table 3 we have tabulated the values our a posteriori error estimator η. Note that in both cases, the convergence rate is approximately $r\approx 2$, as suggested by Theorem 2.1 and Corollary 3.1.

4.2 L-shaped domain

In our second example we remove the bottom left quadrant of the square, and consider the L-shaped domain $(-1,1)\times(-1,1)\backslash[-1,0]\times[-1,0]$, again with homogenous Dirichlet conditions for the velocity, see Figure 1. The results from the calculations are shown in Tables 4– 6.

For the L-shaped domain, the convergence rates of the exact and estimated errors vary in the range $1.7\le r\le 2$, depending on the regularity of

Mode/N	4	8	16	32	64	128	ref
1	18.403	14.377	13.400	13.164	13.105	13.091	13.086
2	33.716	25.879	23.730	23.204	23.074	23.042	23.031
3	41.929	27.676	24.143	23.304	23.099	23.048	23.031
4	53.024	39.937	34.078	32.555	32.177	32.084	32.053
5	79.801	47.721	40.783	39.087	38.669	38.566	38.532
6	91.089	52.290	44.193	42.351	41.905	41.794	41.759
7	125.123	59.801	50.673	48.214	47.597	47.444	47.393
8	128.224	67.366	52.419	48.626	47.698	47.469	47.393
9	152.065	81.101	66.333	62.742	61.869	61.652	61.583
10	155.823	83.846	67.104	62.928	61.915	61.664	61.583

Table 1: Numerical eigenvalues λ_h for $h = \sqrt{2/N}$ and the extrapolated reference solution λ for the unit square.

Mode/N	4	8	16	32	64	128	rate
1	0.4063	0.0986	0.0240	0.0059	0.0015	0.0004	2.020
2	0.4639	0.1236	0.0303	0.0075	0.0018	0.0005	2.018
3	0.8205	0.2017	0.0482	0.0118	0.0029	0.0007	2.026
4	0.6543	0.2460	0.0632	0.0157	0.0039	0.0010	2.012
5	1.0710	0.2385	0.0584	0.0144	0.0036	0.0009	2.019
6	1.1813	0.2522	0.0583	0.0142	0.0035	0.0008	2.036
7	1.6401	0.2618	0.0692	0.0173	0.0043	0.0011	2.000
8	1.7055	0.4214	0.1060	0.0260	0.0064	0.0016	2.026
9	1.4693	0.3169	0.0771	0.0188	0.0046	0.0011	2.032
10	1.5303	0.3615	0.0896	0.0218	0.0054	0.0013	2.034

Table 2: Errors $|\lambda - \lambda_h|/\lambda$ and the convergence rate r for the unit square.

Mode/N	4	8	16	32	64	128	rate
1	1.7204	0.1325	0.0996	0.0255	0.0065	0.0016	1.976
2	3.2066	0.1360	0.1542	0.0394	0.0100	0.0025	1.979
3	4.7796	0.1581	0.1821	0.0462	0.0117	0.0030	1.982
4	5.7537	0.1498	0.2569	0.0657	0.0167	0.0042	1.977
5	9.9275	0.1535	0.2652	0.0668	0.0169	0.0043	1.986
6	13.1493	0.1669	0.2806	0.0694	0.0175	0.0044	1.998
7	18.3303	0.1443	0.3406	0.0868	0.0220	0.0056	1.979
8	18.3590	0.1632	0.4001	0.1002	0.0253	0.0064	1.990
9	22.9004	0.1686	0.3991	0.0975	0.0245	0.0062	2.005
10	5.3907	0.1446	0.4223	0.1028	0.0258	0.0065	2.006

Table 3: Estimated errors η and the convergence rate r for the unit square.

Mode/N	4	8	16	32	64	128	ref
1	61.122	43.131	35.216	33.086	32.461	32.257	32.1734
2	89.147	46.312	39.322	37.608	37.172	37.058	37.0199
3	127.47	53.878	44.962	42.704	42.137	41.993	41.9443
4	139.01	65.379	53.182	50.024	49.242	49.048	48.9844
5	189.86	79.876	62.313	57.198	55.895	55.553	55.4365
6	195.10	100.55	78.836	72.010	70.223	69.733	69.5600
7	205.99	108.18	79.029	72.682	71.143	70.760	70.6382
8	213.28	124.04	93.381	85.350	83.245	82.683	82.4832
9	213.85	127.10	93.951	86.028	84.086	83.599	83.4450
10	215.09	143.23	103.93	92.914	90.176	89.490	89.2902

Table 4: Numerical eigenvalues λ_h for $h = \sqrt{2/N}$ and the extrapolated reference solution λ for the L-shaped domain.

Mode/N	4	8	16	32	64	128	rate
1	0.8998	0.3406	0.0946	0.0284	0.0089	0.0026	1.7214
2	1.4081	0.2510	0.0622	0.0159	0.0041	0.0010	1.9650
3	2.0390	0.2845	0.0719	0.0181	0.0046	0.0012	1.9864
4	1.8378	0.3347	0.0857	0.0212	0.0053	0.0013	2.0130
5	2.4248	0.4409	0.1240	0.0318	0.0083	0.0021	1.9596
6	1.8048	0.4455	0.1334	0.0352	0.0095	0.0025	1.9525
7	1.9161	0.5315	0.1188	0.0289	0.0071	0.0017	2.0329
8	1.5857	0.5038	0.1321	0.0348	0.0092	0.0024	1.9228
9	1.5628	0.5232	0.1259	0.0310	0.0077	0.0018	2.0182
10	1.4089	0.6041	0.1640	0.0406	0.0099	0.0022	2.0612

Table 5: Errors $|\lambda - \lambda_h|/\lambda$ and the convergence rate r for the L-shaped domain.

the corresponding eigenfunction (see Theorem 2.1 and the analysis of MINI element [6] for more details). Nevertheless, the tables show that estimator η is optimal in the sense that it always has approximately the same convergence rate as the true error with respect to the reference solution.

4.3 Adaptive refinement for the L-shaped domain

The software Elmer [11] uses a error balancing strategy. First, a a coarse starting mesh is prescribed. Then, after computing the approximate solution and the corresponding error estimators, a complete remeshing is done by using a Delaunay triangulation. The refining–coarsening strategy is based on the local error indicators and on the assumption that the local error is of the form

$$\eta_K = C_K h_K^{p_K}, \tag{3}$$

Mode/N	4	8	16	32	64	128	rate
1	2.3135	0.2992	0.0606	0.0200	0.0067	0.0023	1.7058
2	3.4751	0.2133	0.0164	0.0095	0.0026	0.0007	1.9496
3	5.9479	0.2334	0.0136	0.0077	0.0020	0.0006	1.9413
4	7.0110	0.2472	0.0126	0.0055	0.0009	0.0003	1.9805
5	13.152	0.3049	0.0175	0.0129	0.0041	0.0015	1.9007
6	15.547	0.3969	0.0139	0.0226	0.0072	0.0024	1.8516
7	24.925	0.7347	0.0248	0.0075	0.0014	0.0004	1.9822
8	25.973	0.6432	0.0155	0.0172	0.0050	0.0018	1.8920
9	28.716	0.7081	0.0167	0.0120	0.0031	0.0008	1.9752
10	35.779	0.6366	0.0157	0.0127	0.0038	0.0012	1.9608

Table 6: Estimated errors η and the convergence rate r for the L-shaped domain.

for some constants C_K and p_K. The new mesh is then built with the aim of having the error uniformly distributed over the elements.

The stopping criteria for the adaptive process is either a given tolerance for the maximum local estimator or the number of refinement steps. Between two subsequent adaptive steps we have used the value 2 for the change of the relative local mesh density ratio. For the element size, neither a maximum nor a minimum have been prescribed.

The sequence of meshes is shown in Figure 2. In Figure 3 the error estimator is plotted as a function of the number of degrees of freedom for the adaptive scheme and the uniform refinement.

Acknowledgements

This work has been supported by TEKES, the National Technology Agency of Finland, in the context of the project KOMASI (decision number 40288/05).

References

[1] M. Ainsworth and J. T. Oden, *A posteriori error estimation in finite element analysis*, Pure and Applied Mathematics (New York), Wiley-Interscience [John Wiley & Sons], New York, 2000.

[2] D. N. Arnold and F. Brezzi, *Mixed and nonconforming finite element methods: implementation, postprocessing and error estimates*, RAIRO Modél. Math. Anal. Numér., 19 (1985), pp. 7–32.

[3] I. Babuška and J. Osborn, *Eigenvalue problems*, in Handbook of Numerical Analysis, Vol. II, North-Holland, Amsterdam, 1991, pp. 641–787.

[4] D. Boffi, F. Brezzi, and L. Gastaldi, *On the convergence of eigenvalues for mixed formulations*, Ann. Scuola Norm. Sup. Pisa Cl. Sci. (4), 25 (1997), pp. 131–154 (1998).

[5] D. Braess, *Finite Elements. Theory, Fast Solvers, and Applications in Solid Mechanics*, Cambridge University Press, 1997.

[6] F. Brezzi and M. Fortin, *Mixed and hybrid finite element methods*, vol. 15 of Springer Series in Computational Mathematics, Springer-Verlag, New York, 1991.

[7] P. G. Ciarlet, *The finite element method for elliptic problems*, vol. 40 of Classics in Applied Mathematics, Society for Industrial and Applied Mathematics (SIAM), Philadelphia, PA, 2002. Reprint of the 1978 original [North-Holland, Amsterdam; MR0520174 (58 #25001)].

[8] W. Dörfler and M. Ainsworth, *Reliable a posteriori error control for nonconformal finite element approximation of Stokes flow*, Math. Comp., 74 (2005), pp. 1599–1619 (electronic).

[9] R. G. Durán, L. Gastaldi, and C. Padra, *A posteriori error estimators for mixed approximations of eigenvalue problems*, Math. Models Methods Appl. Sci., 9 (1999), pp. 1165–1178.

[10] R. G. Durán, C. Padra, and R. Rodríguez, *A posteriori error estimates for the finite element approximation of eigenvalue problems*, Math. Models Methods Appl. Sci., 13 (2003), pp. 1219–1229.

[11] Elmer finite element software homepage. `http://www.csc.fi/elmer`.

[12] E. B. Fabes, C. E. Kenig, and G. C. Verchota, *The Dirichlet problem for the Stokes system on Lipschitz domains*, Duke Math. J., 57 (1988), pp. 769–793.

[13] V. Heuveline and R. Rannacher, *A posteriori error control for finite approximations of elliptic eigenvalue problems*, Adv. Comput. Math., 15 (2001), pp. 107–138 (2002).

[14] M. G. Larson, *A posteriori and a priori error analysis for finite element approximations of self-adjoint elliptic eigenvalue problems*, SIAM J. Numer. Anal., 38 (2000), pp. 608–625 (electronic).

[15] B. Mercier, J. Osborn, J. Rappaz, and P.-A. Raviart, *Eigenvalue approximation by mixed and hybrid methods*, Math. Comp., 36 (1981), pp. 427–453.

[16] G. Savaré, *Regularity results for elliptic equations in Lipschitz domains*, J. Funct. Anal., 152 (1998), pp. 176–201.

[17] L. R. Scott and S. Brenner, *The Mathematical Theory of Finite Element Methods*, Springer-Verlag, 1994.

[18] R. Verfürth, *A Review of A Posteriori Error Estimation and Adaptive Mesh-Refinement Techniques*, Wiley-Teubner, 1996.

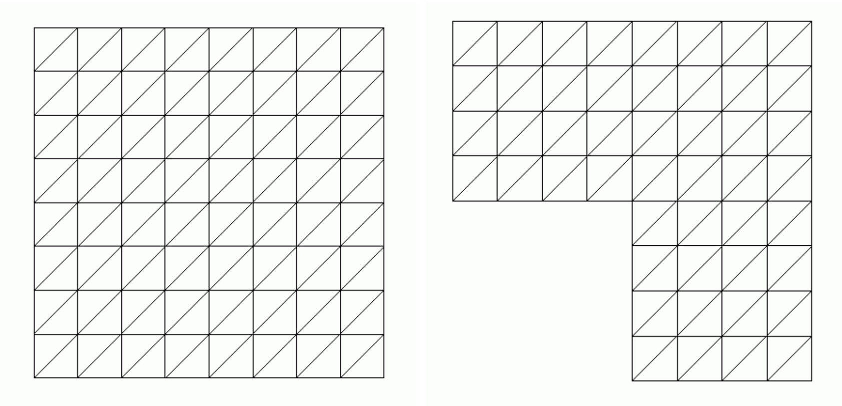

Figure 1: Uniform finite element partitioning of the unit square and L-shaped domain for $N = 8$.

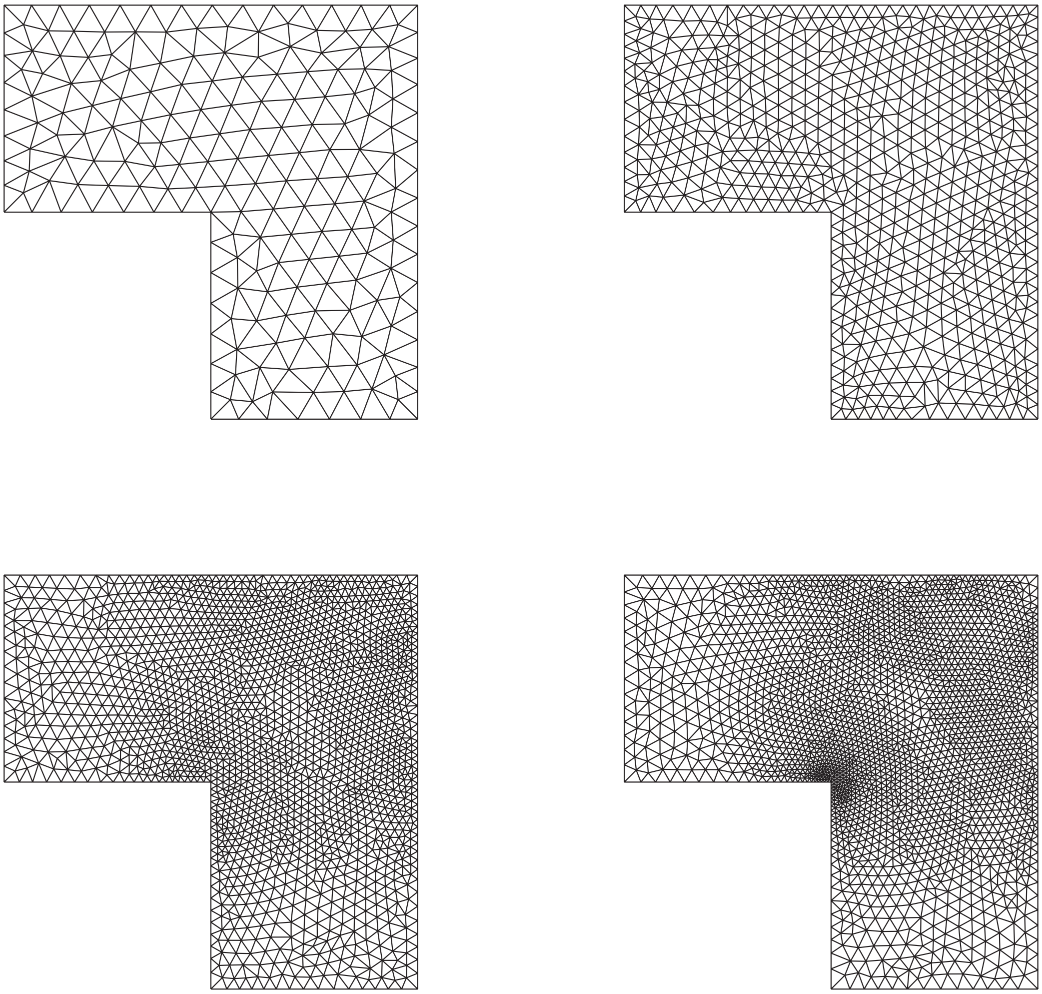

Figure 2: The sequence of adaptive mesh refinement for the smallest eigenvalue of the Stokes operator in the L-shaped domain.

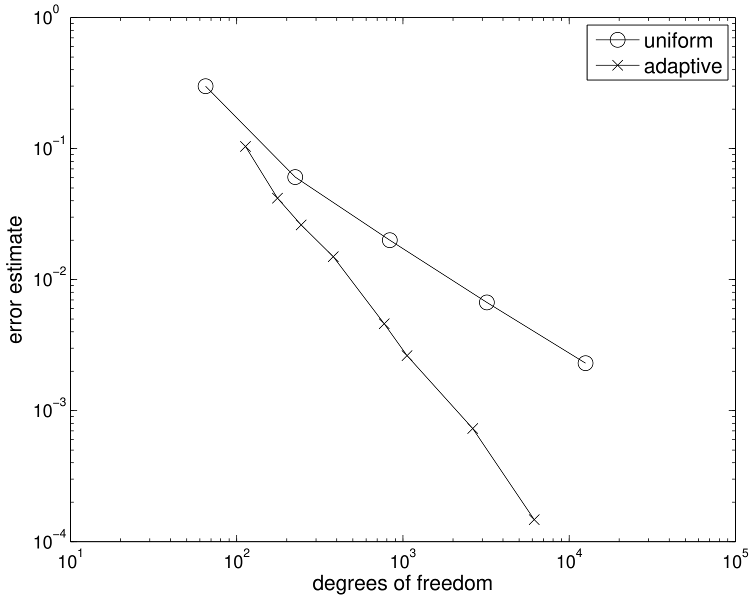

Figure 3: Error estimate for adaptive and uniform mesh refinement.

(continued from the back cover)

HELSINKI UNIVERSITY OF TECHNOLOGY INSTITUTE OF MATHEMATICS
RESEARCH REPORTS

The list of reports is continued inside. Electronical versions of the reports are available at *http://math.tkk.fi/reports/* .

A516 Sergey Repin , Rolf Stenberg
Two-sided a posteriori estimates for the generalized stokes problem
December 2006

A515 Sergey Korotov
Global a posteriori error estimates for convection-reaction-diffusion problems
December 2006

A514 Yulia Mishura , Esko Valkeila
An extension of the L'evy characterization to fractional Brownian motion
December 2006

A513 Wolfgang Desch , Stig-Olof Londen
On a Stochastic Parabolic Integral Equation
October 2006

A512 Joachim Schöberl , Rolf Stenberg
Multigrid methods for a stabilized Reissner-Mindlin plate formulation
October 2006

ISBN-13 978-951-22-8456-6
ISBN-10 951-22-8456-1